

**TOWARDS IMPROVED ESTIMATES OF GLOBAL CLOUD
FRACTION BY ADDRESSING UNCERTAINTIES INVOLVED
IN SATELLITE CLOUD REMOTE SENSING**

SOUMI DUTTA



**CENTRE FOR ATMOSPHERIC SCIENCES
INDIAN INSTITUTE OF TECHNOLOGY DELHI**

JUNE 2023

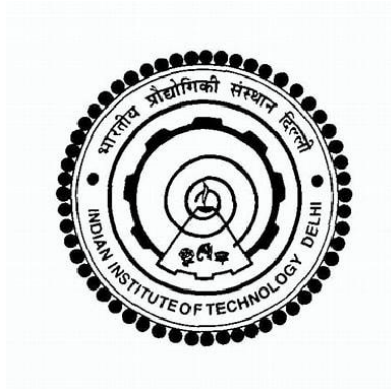
© Indian Institute of Technology Delhi (IITD), New Delhi, 2023

**Towards Improved Estimates of Global Cloud Fraction
by Addressing Uncertainties Involved in Satellite Cloud
Remote Sensing**

by
Soumi Dutta

Centre for Atmospheric Sciences

submitted
in fulfilment of the requirements of the degree of Doctor of Philosophy
to the

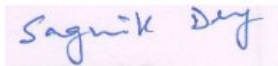


Indian Institute of Technology Delhi

June 2023

Certificate

This is to certify that the thesis entitled “Towards Improved Estimates of Global Cloud Fraction by Addressing Uncertainties Involved in Satellite Cloud Remote Sensing” is being submitted by Soumi Dutta for the award of the degree of Doctor of Philosophy, is a record of the original bonafide research work carried out by her. She has worked under my guidance and supervision and has fulfilled the requirements for submitting this thesis. The results presented in this thesis have not been submitted in part or whole to any University or Institution for the award of any degree/diploma.



Prof. Sagnik Dey

Professor

**Centre for Atmospheric Sciences,
Indian Institute of Technology Delhi,
Hauz Khas, New Delhi-110016, India**



Prof. Larry Di Girolamo

Professor

**Department of Atmospheric Sciences,
University of Illinois at Urbana-Champaign
Urbana, IL-61801, USA**

Acknowledgments

Completing any work we take up in life is always a team effort. This thesis is no different. I want to express my sincere gratitude to my thesis supervisors, Prof. Sagnik Dey (IIT Delhi) and Prof. Larry Di Girolamo (UIUC), for allowing me to pursue a Ph.D. under their supervision. I am grateful for their invaluable guidance, constructive criticism, and constant encouragement. I benefited from their subject expertise and academic experience, making my Ph.D. tenure enlightening, cheerful and motivating. They have always allowed me to pursue my interests and provided me with insightful suggestions and support in developing independent thinking and research skills.

I sincerely thank my SRC (Student Research Committee) members for generously sharing their knowledge and time. I would also like to thank the Head of the Centre, my CRC (Centre Research Committee) chairperson, and all the faculties and staff at the Centre for Atmospheric Sciences (CAS), IIT Delhi, for providing all the necessary facilities and a great environment to learn and grow. During my Ph.D. tenure, they are always available for discussion, suggestions, and other academic and non-academic help. I am grateful to Prof. Larry Di Girolamo and Prof. Sagnik Dey for allowing me to visit UIUC for nine months during my Ph.D. and pursue my research there under their expert guidance.

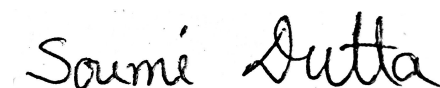
I want to acknowledge the High-performance computing (HPC) facilities at IITD and the National Center for Supercomputing Applications (NCSA) facilities at UIUC for providing the required computing facilities for extensive satellite data handling during my Ph.D. tenure. I also like to acknowledge the computing and storage facilities at CAS, IIT Delhi, for hassle-free computation and analysis during my Ph.D. I thank the IITD Institute fellowship for funding my

Ph.D. research at IITD, and MISR project (under contract 1474871), and NASA (National Aeronautics and Space Administration) ACCESS program (contract NNX16AM07A) for supporting my stay and research at UIUC.

I want to thank my friends, hostel mates, and labmates from IIT Delhi and UIUC for always being friends in need, and their excellent company made my stay at IITD and UIUC pleasant and memorable. I also thank the AINA (An Initiative to National Advancement), SPICMACAY (The Society for the Promotion of Indian Classical Music And Culture Amongst Youth) clubs, and Kailash Hostel at IITD for being part of my life during the Ph.D. period. My sincere thanks to the Indian Graduate Students Association, UIUC, for helping me find my stay in the USA.

Words cannot completely express my love and gratitude to my family members who have supported and encouraged me through this journey. I thank them for making all the efforts to nurture me. My parents were my first teachers. They scolded and molded me as a girl child and gave me the freedom to become a complete woman.

I strongly believe in 'pronoia', that is, 'When you want something, all the Universe conspires to help you to achieve it'. So, the final acknowledgement is dedicated to the almighty God and the Universe for providing me the passion, strength, perseverance, resources, and patience to complete the highest academic degree.

A handwritten signature in black ink that reads "Soumi Dutta". The signature is written in a cursive, flowing style.

June 2023

Soumi Dutta

Abstract

Clouds play an important role in modulating Earth's radiation balance and hydrological cycle. The response of clouds to global climate is considered one of the most considerable uncertainties in climate prediction. To minimize the significant uncertainty in the climate models, accurate measurement of cloud fraction (CF) or cloudiness is the first and foremost requirement. Since CF's 'true' global distribution can not be obtained from ground-based measurements, satellite remote sensing is the only tool to get the global distribution of cloudiness at a continuous scale for a long-term period. However, considerable disagreements exist in the measurements of CF among various satellites, making it difficult to use them to evaluate and improve climate model predictions. Major causes for discrepancies among satellite derived CFs are (a) finite scale of cloud detection ('resolution effect'), (b) viewing geometry of sensors ('view angle effect'), (c) 'diurnal cycle' effect, and (d) 'instrument sensitivity and cloud detection methodology' effect. The only way to have a more realistic estimate of global CF is to minimize the uncertainties mentioned in satellite cloud remote sensing. In this thesis, the causes mentioned above for discrepancies in satellite cloud remote sensing have been addressed toward improved estimates of global cloud coverage.

Passive remote sensing instrument Multi-angle Imaging SpectroRadiometer (MISR) uses 'clear-conservative cloud masking' to detect a pixel as "cloudy" if it contains any subpixel level cloud defined. This factor causes the 'resolution effect' present in MISR CF. A pattern recognition technique algorithm has been included in the MISR standard CF product to correct CF's 'resolution effect' bias since 2014 but was yet to be assessed. In this thesis, the resolution-corrected MISR CF product has been assessed to answer whether an improved estimate of near-global (50N-50S) cloud coverage has been achieved after this resolution effect correction. The study shows a large

reduction (up to ~ 0.4) in MISR CF after resolution correction is applied using the pattern recognition technique. New MISR resolution-corrected CF is observed to be within ± 0.05 - 0.08 of ASTER (Advanced Spaceborne Thermal Emission and Reflection Radiometer) CF which is considered a 'true' CF because of its' very high pixel resolution (15m).

MODIS (Moderate Resolution Imaging Spectroradiometer), a passive remote sensing instrument, has a broader swath width of 2,330 km than MISR's much narrower swath of 360 km. This fact causes the dependencies of MODIS cloud properties on its viewing geometry which is undesirable but inevitable. The present thesis has corrected the 'view-angle effect' in MODIS CF. Near-global cloud cover has been reduced from 0.66 to 0.59 after the view-angle correction was applied to MODIS data for all seasons. Ground-based observations also have a viewing geometry effect in measuring cloud cover. The 'view-angle effect' has been corrected for the ground-based observation data (EECRA - Extended Edited Synoptic Cloud Reports Archive). Like MODIS, here also, CF is reduced after view-angle correction, and the reduction happens from 0.61 to 0.57 on an annual scale.

Improved understanding of atmospheric circulation processes demands accurate knowledge about height-stratified cloud amounts and cloud vertical structure. However, because of the existing uncertainties among sensors to detect high, mid, and low clouds, explicit knowledge about the vertical distribution of clouds seems elusive. The present thesis examines the state-of-the-art long-term passive and active CF data products and the ground-based observation to examine their strengths and weaknesses in detecting clouds at different altitudes. It is evident from the study that no single dataset can be treated as the 'true' source of height-stratified CF as some sensors are good

at detecting low clouds while others are sensitive to high ones. Broadly, it has been found that high level clouds are best observed by CALIPSO-GOCCP (GCM-Oriented Cloud-Aerosol Lidar and Infrared Pathfinder Satellite Observation) among active remote sensors and by ISCCP (International Satellite Cloud Climatology Project) among passive sensors. MISR is good at detecting low level clouds which are well observed by CloudSat radar and ground-based observation. The results of this chapter are consistent with previous studies but provide new insights about the height-stratification and vertical distribution of clouds.

Observation at a very high temporal resolution is needed to monitor highly variable parameters like fractional cloud coverage. Using observations only from sun-synchronous or polar orbiting satellites can not be used directly to study the cloud dynamics because their time sampling is too infrequent to capture the evolution of cloud systems. To overcome this issue, continuous observations are required from geostationary satellites, capable of providing information at a very high temporal resolution. In the present thesis, the diurnal scale signature of cloud coverage has been studied, focusing on the geostationary satellite Kalpana-1 over the south Asian monsoon region. It has been found that the Indian meteorological satellite Kalpana-1 has well observed the diurnal scale signature of total CF over the Indian subcontinent. Amplitude and local time of maximum CF show seasonal and spatial variability over the land and oceanic regions. Kalpana-1 CF has been assessed against MISR resolution-corrected CF and found positively correlated with the new MISR CF.

This thesis work thus addresses all the above mentioned uncertainties involved in satellite cloud remote sensing to get improved cloud cover estimates. Once the CF climatology from various

datasets converges after correcting these uncertainties, it will be more prudent to fuse multiple datasets according to their strengths and derive a unified global height-stratified cloud climatology. The outcome of this PhD thesis work is a step forward toward improved estimates of global cloud fraction climatology, which is an important step for an accurate estimate of Earth's radiation budget.

सारांश

बादल पृथ्वी के विकिरण संतुलन और हाइड्रोलॉजिकल चक्र को संशोधित करने में महत्वपूर्ण भूमिका निभाते हैं। वैश्विक जलवायु के लिए बादलों की प्रतिक्रिया को जलवायु पूर्वानुमान में सबसे महत्वपूर्ण अनिश्चितताओं में से एक माना जाता है। जलवायु मॉडल में महत्वपूर्ण अनिश्चितता को कम करने के लिए, सटीक क्लाउड अंश (सीएफ) या बादल की माप पहली और सबसे महत्वपूर्ण आवश्यकता है। क्योंकि सीएफ का 'सही' वैश्विक वितरण जमीन-आधारित माप से प्राप्त नहीं किया जा सकता है, उपग्रह रिमोट सेंसिंग लंबे समय तक निरंतर पैमाने पर बादलों के वैश्विक वितरण को प्राप्त करने का एकमात्र उपकरण है। हालांकि, विभिन्न उपग्रहों के बीच सीएफ के माप में काफी असहमति मौजूद है, जो जलवायु मॉडल भविष्यवाणियों का मूल्यांकन और सुधार करने के लिए उनका उपयोग करना मुश्किल बनाता है। उपग्रह व्युत्पन्न सीएफ के बीच विसंगतियों के प्रमुख कारण हैं (क) क्लाउड डिटेक्शन का परिमित पैमाना ('रिज़ॉल्यूशन प्रभाव'), (ख) सेंसर की ज्यामिति देखना ('दृश्य कोण प्रभाव'), (ग) 'दैनिक चक्र' प्रभाव, और (घ) उपकरण संवेदनशीलता और क्लाउड डिटेक्शन पद्धति का प्रभाव। वैश्विक सीएफ का अधिक यथार्थवादी अनुमान लगाने का एकमात्र तरीका है उपग्रह क्लाउड रिमोट सेंसिंग में उल्लिखित अनिश्चितताओं को कम करना। इस थीसिस में, उपग्रह क्लाउड रिमोट सेंसिंग में विसंगतियों के लिए ऊपर उल्लिखित कारणों को वैश्विक क्लाउड कवरेज के बेहतर अनुमानों की ओर संबोधित किया गया है।

निष्क्रिय रिमोट सेंसिंग उपकरण मल्टी-एंगल इमेजिंग स्पेक्ट्रोरेडियोमीटर (एमआईएसआर) किसी पिकसेल को "बादल" के रूप में पहचानने के लिए 'क्लियर कंज़रवेटिव क्लाउड मास्किंग' का उपयोग करता है यदि इसमें कोई उपपिकसेल स्तर का क्लाउड होता है। यह कारक एमआईएसआर सीएफ में मौजूद 'रिज़ॉल्यूशन प्रभाव' का कारण बनता है। 2014 से सीएफ के 'रिज़ॉल्यूशन प्रभाव' पूर्वाग्रह को ठीक करने के लिए एमआईएसआर मानक सीएफ उत्पाद में एक पैटर्न मान्यता तकनीक एल्गोरिदम शामिल किया गया है, लेकिन अभी तक मूल्यांकन नहीं किया गया था। इस थीसिस में, रिज़ॉल्यूशन-सही एमआईएसआर सीएफ उत्पाद का मूल्यांकन यह उत्तर देने के लिए किया गया है कि क्या इस

रिज़ॉल्यूशन प्रभाव सुधार के बाद निकट-वैश्विक (50 एन -50 एस) क्लाउड कवरेज का एक बेहतर अनुमान हासिल किया गया है। अध्ययन से पता चलता है पैटर्न पहचान तकनीक का उपयोग करके रिज़ॉल्यूशन सुधार लागू करने के बाद एमआईएसआर सीएफ कमी (~0.4 तक)। नए एमआईएसआर रिज़ॉल्यूशन-सही सीएफ को एएसटीईआर (एडवांस्ड स्पेसबोर्न थर्मल एमिशन एंड रिप्लेक्शन रेडियोमीटर) सीएफ के $\pm 0.05-0.08$ के भीतर पाया गया है। इसके 'बहुत उच्च पिक्सेल रिज़ॉल्यूशन (15 मीटर) के कारण इसे 'सच्चा' सीएफ माना जाता है।

एमओडीआईएस (मॉडरेट रिजोल्यूशन इमेजिंग स्पेक्ट्रोरेडियोमीटर), एक निष्क्रिय रिमोट सेंसिंग उपकरण, एमआईएसआर की 360 किमी की बहुत संकरी पट्टी की तुलना में 2,330 किमी की व्यापक पट्टी की चौड़ाई है। यह तथ्य इसकी देखने की ज्यामिति पर एमओडीएस क्लाउड गुणों की निर्भरता का कारण बनता है जो अवांछनीय लेकिन अपरिहार्य है। वर्तमान थीसिस ने एमओडीआईएस सीएफ में 'व्यू-एंगल इफेक्ट' को सही किया है। सभी मौसमों के लिए एमओडीआईएस डेटा पर दृश्य-कोण सुधार लागू होने के बाद निकट-वैश्विक क्लाउड कवर 0.66 से घटकर 0.59 हो गया है। बादल कवर को मापने में जमीन-आधारित अवलोकनों का ज्यामिति प्रभाव भी होता है। ग्राउंड-आधारित अवलोकन डेटा (ईईसीआरए - विस्तारित संपादित सिनॉप्टिक क्लाउड रिपोर्ट आर्काइव) के लिए 'व्यू-एंगल इफेक्ट' को ठीक किया गया है। एमओडीआईएस की तरह, यहां भी, दृश्य-कोण सुधार के बाद सीएफ कम हो जाता है, और कमी वार्षिक पैमाने पर 0.61 से 0.57 तक होती है।

वायुमंडलीय परिसंचरण प्रक्रियाओं की बेहतर समझ ऊंचाई-स्तरीकृत क्लाउड मात्रा और क्लाउड ऊर्ध्वाधर संरचना के बारे में सटीक ज्ञान की मांग करती है। हालांकि, उच्च, मध्य और निम्न बादलों का पता लगाने के लिए सेंसर के बीच मौजूदा अनिश्चितताओं के कारण, बादलों के ऊर्ध्वाधर वितरण के बारे में स्पष्ट ज्ञान मुश्किल लगता है। वर्तमान थीसिस विभिन्न ऊंचाई पर बादलों का पता लगाने में उनकी ताकत और कमजोरियों की जांच करने के लिए अत्याधुनिक दीर्घकालिक निष्क्रिय और सक्रिय सीएफ डेटा उत्पादों और जमीन-आधारित अवलोकन की जांच करती है। अध्ययन से यह स्पष्ट है कि किसी भी डेटासेट को ऊंचाई-स्तरीकृत सीएफ के 'सही' स्रोत के रूप में नहीं माना जा

सकता है क्योंकि कुछ सेंसर कम बादलों का पता लगाने में अच्छे होते हैं जबकि अन्य उच्च बादलों के प्रति संवेदनशील होते हैं। मोटे तौर पर, यह पाया गया है कि उच्च स्तरीय बादलों को सक्रिय रिमोट सेंसर के बीच कैलिप्सो जीओसीसीपी (जीसीएम-ओरिंटेड क्लाउड-एयरोसोल लिडार और इन्फ्रारेड पाथफाइंडर सैटेलाइट ऑब्जर्वेशन) द्वारा और निष्क्रिय सेंसर के बीच आईएससीसीपी (इंटरनेशनल सैटेलाइट क्लाउड क्लाइमेटोलॉजी प्रोजेक्ट) द्वारा सबसे अच्छा देखा जाता है। एमआईएसआर निम्न स्तर के बादलों का पता लगाने में अच्छा है जो क्लाउडसैट रडार और जमीन-आधारित अवलोकन द्वारा अच्छी तरह से देखे जाते हैं। इस अध्याय के परिणाम पिछले अध्ययनों के अनुरूप हैं, लेकिन बादलों की ऊंचाई-स्तरीकरण और ऊर्ध्वाधर वितरण के बारे में नई अंतर्दृष्टि प्रदान करते हैं।

आंशिक क्लाउड कवरेज जैसे अत्यधिक परिवर्तनीय मापदंडों की निगरानी के लिए बहुत उच्च टेम्परल रिज़ॉल्यूशन पर अवलोकन की आवश्यकता होती है। केवल सूर्य-तुल्यकालिक या ध्रुवीय परिक्रमा उपग्रहों से अवलोकनों का उपयोग क्लाउड गतिशीलता का अध्ययन करने के लिए सीधे नहीं किया जा सकता है क्योंकि क्लाउड सिस्टम के विकास को पकड़ने के लिए उनका समय नमूनाकरण बहुत कम है। इस मुद्दे को दूर करने के लिए, भूस्थिर उपग्रहों से निरंतर अवलोकन की आवश्यकता होती है, जो बहुत उच्च टेम्परल रिज़ॉल्यूशन पर जानकारी प्रदान करने में सक्षम हैं। वर्तमान थीसिस में, दक्षिण एशियाई मानसून क्षेत्र पर भूस्थिर उपग्रह कल्पना -1 पर ध्यान केंद्रित करते हुए क्लाउड कवरेज के दैनिक पैमाने के हस्ताक्षर का अध्ययन किया गया है। यह पाया गया है कि भारतीय मौसम विज्ञान उपग्रह कल्पना -1 ने भारतीय उपमहाद्वीप पर कुल सीएफ के दैनिक पैमाने के हस्ताक्षर को अच्छी तरह से देखा है। अधिकतम सीएफ के आयाम और स्थानीय समय भूमि और समुद्री क्षेत्रों पर मौसमी और स्थानिक परिवर्तनशीलता दिखाते हैं। कल्पना -1 सीएफ का मूल्यांकन एमआईएसआर रिज़ॉल्यूशन-सही सीएफ के साथ किया गया है और नए एमआईएसआर सीएफ के साथ सकारात्मक रूप से सहसंबद्ध पाया गया है।

इस प्रकार यह थीसिस कार्य बेहतर क्लाउड कवर अनुमान प्राप्त करने के लिए उपग्रह क्लाउड रिमोट सेंसिंग में शामिल उपरोक्त सभी अनिश्चितताओं को संबोधित करता है। एक बार जब विभिन्न डेटासेट से सीएफ जलवायु विज्ञान इन अनिश्चितताओं को ठीक करने के बाद अभिसरण करता है, तो कई डेटासेट को उनकी ताकत के अनुसार फ्यूज करना और एक एकीकृत वैश्विक ऊंचाई-स्तरीकृत क्लाउड क्लाइमेटोलॉजी प्राप्त करना अधिक विवेकपूर्ण होगा। इस पीएचडी थीसिस कार्य का परिणाम वैश्विक क्लाउड अंश जलवायु विज्ञान के बेहतर अनुमानों की दिशा में एक कदम आगे है, जो पृथ्वी के विकिरण बजट के सटीक अनुमान के लिए एक महत्वपूर्ण कदम है।

Contents

Certificate	i
Acknowledgements	iii
Abstract	v
Hindi Abstract	ix
Contents	xiii
List of Figures	xvii
List of Tables	xx
Chapter 1: Introduction	1
1.1 Importance of clouds in climate science	3
1.2 Importance of cloud fraction	3
1.3 Various ways of estimating global cloud fraction	5
1.3.1 Climate models	5
1.3.2 Surface observation	7
1.3.3 Satellite Remote Sensing	9
1.3.3.1 Types of satellite remote sensing	9
1.3.3.2 Satellite remote sensing of clouds	10
1.3.3.3 Disagreement among satellites in detection of clouds	10
1.4 Global cloud climatology derived from satellites and ground-based remote sensing	11
1.5 Research gaps and motivation	13
1.6 Thesis objectives and thesis structure	14

Chapter 2: Addressing Uncertainties due to ‘Finite Spatial Resolution’ of Sensors in	
Detecting Clouds	15
2.1 What is the finite ‘resolution effect’ and how does it affect calculation of cloud fraction?	17
2.2 Spatial pattern matters most in ‘resolution effect’	19
2.3 Correction and assessment of the finite ‘resolution effect’ in MISR cloud fraction	20
2.4 Data and methods	21
2.4.1 Datasets used	21
2.4.2 MISR data and analysis	21
2.4.3 ASTER data and analysis	23
2.4.4 MISR-ASTER collocation	26
2.5 Results	26
2.5.1 Changes in MISR cloud fraction after resolution-effect correction	26
2.5.2 Evaluation against ‘true’ cloud fraction derived from ASTER data	30
2.6 Summary	33
Chapter 3: Quantification and Minimization the ‘View-angle effect’ in Global Cloud	
Climatology	35
3.1 View angle effect on calculation of cloud fraction in MODIS	37
3.2 View angle effect on calculation of cloud fraction in surface observation	39
3.3 Correction of ‘view-angle effect’ in MODIS CF and surface-based estimated CF	40
3.3.1 Datasets used	40
3.3.2 MODIS data and analysis	41
3.3.3 ASTER, MISR, and MODIS Collocation	43
3.3.4 Surface station based data and analysis	43

3.4 Results	44
3.4.1 Changes in cloud fraction after view-angle correction in MODIS	44
3.4.2 Changes in cloud fraction after view-angle correction in surface-based observation	45
3.4.3 Evaluation of ‘view-angle’ corrected MODIS CF against the ‘true’ ASTER and the ‘resolution-corrected’ MISR CF	47
3.5 Summary	49

Chapter 4 : Comparative Assessment of the ‘Height-stratified’ Global Cloud

Distribution from Active and Passive Remote Sensing Perspective	51
4.1 Height-stratified cloud amounts	53
4.2 Cloud vertical structure	54
4.3 Data and Methods	55
4.3.1 MISR CFbA	56
4.3.2 ISCCP H-series product	57
4.3.3 CALIPSO-GOCCP	58
4.3.4 CloudSat-CALIPSO	59
4.3.5 Ground-based Observation	60
4.4 Results	60
4.4.1 Low level cloud climatology	60
4.4.2 Mid level cloud climatology	63
4.4.3 High level cloud climatology	65
4.4.5 High, mid and low level cloud statistics over land and Ocean	67
4.4.6 Altitude wise zonal mean CF distribution from CloudSat-CALIPSO	69
4.4.7 Altitude wise zonal mean CF distribution from MISR CFbA	72
4.5 Summary	76

Chapter 5: ‘Diurnal Variability’ of Cloudiness over the Indian Subcontinent using Geostationary Satellite Data Product	78
5.1 Diurnal Variability of Cloudiness	80
5.2 Role of satellites in observing diurnal variability of cloudiness	81
5.3 Data and Methods	82
5.3.1 Kalpana-1	83
5.3.2 MISR	83
5.3.3 ISCCP	84
5.5.4 TRMM TMPA	85
5.4 Results	85
5.4.1 Assessment of Kalpana-1 CF against resolution and sunglint corrected MISR CF	85
5.4.2 Kalpana-1 vs ISCCP CF variability in 3-hourly temporal resolution	88
5.4.3 Local time of maximum and amplitude of CF from Kalpana-1	91
5.4.4 Diurnal cycle of CF over specific regions	93
5.4.5 Diurnal variability of cloudiness in active and break phases of monsoon	95
5.5 Summary	98
Chapter 6: Thesis Summary and Future Direction	100
6.1 Summary	102
6.2 Future Direction	107
Abbreviations	109
References	112
Publications	125
Appendix	127

List of Figures

Figure captions	Page No.
Figure 1.1 Variation of net cloud radiative forcing (NETCRF shown by the color scale in $W m^{-2}$) as a function of cloud fraction and cloud optical depth (COD) at different altitudes (represented by cloud top pressure CTP)	4
Figure 1.2: Taylor diagram for mean cloud fraction between individual CMIP6 model and the CALIPSO-CloudSat merged data (a) 20S–20N, (b) 20N–50N, (c) 50N–80N, (d) 20S–50S, (e) 50S–80S, and (f) 80S–80N. Blue indicates the individual model, and the red corresponds to the CMIP6 Ensemble	6
Figure 1.3: Surface Observations of Clouds: Observers see the sides as well as the bases of the clouds	8
Figure 1.4: Global averages of total cloud amount (CA), as well as fraction of high level, mid level, and low level cloud amount relative to the total cloud amount	11
Figure 1.5: Global distribution of total CF from state-of-the-art satellite and ground-based observations	12
Figure 2.1 : Schematic to represent subpixel level ‘cloudy’ and ‘clear’ boxes. Here blue boxes are represented as ‘cloudy’ and ‘white boxes are represented as ‘clear’.	17
Figure 2.2: Variation of mean CF ($\pm 1\sigma$) with degraded pixel resolution. Corresponding standard deviations are shown as error bars.	18
Figure 2.3(a) and 2.3(b): Two ASTER scenes of a $60 km \times 60 km$ area containing different spatial patterns of clouds	19
Figure 2.4: Number of ASTER scenes collected in between the period (02/2000-09/2018). 1 to 6 points denote six regions across the globe where ASTER scenes have been chosen.	24
Figure 2.5. (a) Radiance image generated from DN values (0-255) provided by ASTER L1B data, (b) the corresponding cloud mask and (c) the normalized histogram of DN values. The cloud masking threshold (shown by red line in (c)) for this ASTER scene is 31. Pixels with DN values higher than this thresholds are identified as ‘cloudy’ and lower than the threshold as ‘clear’.	25
Figure 2.6: The first and second column represents the seasonal average of MISR SECF (before resolution correction) and PRCCF (after resolution	27

correction) respectively for DJF, MAM, JJA and SON. The third column shows the absolute changes in MISR CF after the resolution correction (PRCCF-SECF i.e. differences in CF after and before correction).	
Figure 2.7: Probability density distribution of differences in MISR CF after the resolution correction for DJF, MAM, JJA, and SON.	29
Figure 2.8: Mean CF from collocated pixels of ASTER, PRCCF, and SECF over the (a) lands and (b) oceanic regions. (c) represents average values over lands and oceanic regions.	31
Figure 3.1: The mean daytime cloud fraction observations taken from Terra MODIS (a) near nadir (sensor zenith angle between nadir to 10°) and (b) near the edge of scan (sensor zenith angle between 60° to edge of scan)	38
Figure 3.2: The cartoon figure demonstrates how the same amount of CF got overestimated as the sensor viewing geometry changes from the nadir view (the middle one) to the off-nadir edge of the swath view (at the both sides of the sensor swath).	38
Figure 3.3: The earthview (the ideal) of cloud amount is generally less than the satellite view, the surface observer's view and an aircraft view which have 'view-angle effect'.	39
Figure 3.4: (a) A MISR swath of 360 km has been shown inside a wider MODIS swath of 2330 km width. (b) MODIS full swaths of 2330 km in a day (01.01.2015), (c) only daytime MODIS swaths that are within MISR swath width of 360 km i.e., the view-angle corrected ones.	42
Figure 3.5: The first column shows the MODIS CF full swath. the second column is the MODIS CF view-angle corrected (within MISR swath), and the third column is the differences in CF before and after the view-angle correction.	45
Figure 3.6: The first column shows the ground-based observed CF before the view-angle correction applied. the second column is the view-angle corrected ground-based CF. and the third column is the differences in CF before and after the view-angle correction.	46
Figure 3.7: Mean CF from collocated pixels of ASTER, MISR (before and after resolution-correction) and MODIS (after view angle correction) over the lands and oceanic regions.	48
Figure 4.1: Cartoon diagram of multilayer 3D cloud distribution that contains low, mid, and high level clouds.	54
Figure 4.2: Low level cloud distribution from (a) MISR, (b) ISCCP, and (c) CALIPSO-GOCCP, (d) CloudSat-CALIPSO, and (e) Ground-based observations	62-63

Figure 4.3: Mid level cloud distribution from (a) MISR, (b) ISCCP, and (c) CALIPSO-GOCCP, (d) CloudSat-CALIPSO, and (e) Ground-based observations	64-65
Figure 4.4: Low level cloud distribution from (a) MISR, (b) ISCCP, and (c) CALIPSO-GOCCP, (d) CloudSat-CALIPSO, and (e) Ground-based observations	66-67
Figure 4.5: Annual average values of low, mid and high level CF separately over land and ocean on a near-global scale.	68
Figure 4.6: Altitude wise zonal mean CF distribution from joint CloudSat-CALIPSO product over ocean.	70
Figure 4.7: Altitude wise zonal mean CF distribution from joint CloudSat-CALIPSO product over land.	71
Figure 4.8: Altitude wise zonal mean CF distribution from MISR CFbA product over land.	73
Figure 4.9: Altitude wise zonal mean CF distribution from MISR CFbA product over land.	74
Figure 5.1: (a) and (b) show seasonal climatology of total CF at 1030 am over the Indian subcontinent from Kalpana-1 and MISR CFbA. (c) represents the difference plots between CFbA and Kalpana-1, and (d) is Kalpana-1 vs MISR CFbA with calculated correlation coefficient.	87
Figure 5.2: (a) 3-hourly diurnal variation of CF from Kalpana-1 and (b) ISCCP H-series product in JJAS months over the Indian subcontinent.	89
Figure 5.3: Phase (Local time of maximum) of total CF for all seasons (DJF, MAM, JJAS, ON). Local times are in IST (Indian Standard Time).	92
Figure 5.4: Amplitudes (difference between maximum and minimum) of total CF for all seasons (DJF, MAM, JJAS, ON). The regions selected for half-hourly CF analysis are pointed by the boxes in the left-most plot.	93
Figure 5.5: Half-hourly variation of total CF averaged over three oceanic regions (N10-N15, E85-E92 north BoB, N0-N10, E55-E70 south AS , 3-13N, 77-90E South BoB) and two land region (70-88E, 20-25N core monsoon region and 30-40N, 84-94E Tibetan region). Time axis is shown in IST.	95
Figure 5.6: 3-hourly diurnal variation of Kalpana-1 CF during the (a) active and (b) break phase of monsoon.	96-97

List of Tables

Serial Number	Table Caption	Page Number
Table 1.1	Global Annual Average CF Statistics	12
Table 2.1	List of datasets used to address ‘resolution-effect’	21
Table 2.2	MISR CF average (50N-50S) statistics	28
Table 2.3	Mean CFs for the six regions from ASTER, MISR PRCCF and MISR SECF.	33
Table 3.1	List of datasets used to address ‘view-angle’ effect	40
Table 3.2	Summary Table of changes in CF before and after the view angle correction	47
Table 4.1	List of datasets used for comparative assessment of height-stratified CF	56
Table 4.2	Summary table of strengths and weaknesses active, passive, and ground-based remote sensors in detecting multilayer clouds.	75
Table 5.1	List of datasets used to address diurnal variability effect	82